Neutron diffraction study of quasi-one-dimensional lithium purple bronze: Possible mechanism for dimensional crossover

M. S. da Luz, J. J. Neumeier, C. A. M. dos Santos, B. D. White, H. J. Izario Filho, J. B. Leão, and Q. Huang

Phys. Rev. B **84**, 014108 — Published 26 July 2011

DOI: 10.1103/PhysRevB.84.014108

Neutron diffraction study of quasi-one-dimensional lithium purple bronze: possible mechanism for dimensional crossover

J. J. Neumeier,[1] M. S. da Luz,[1,*] C. A. M. dos Santos,[1,2] B. D. White,[1] H. J. I. Filho,[2] J. B. Leão,[3] and Q. Huang[3]

[1]*Department of Physics, P. O. Box 173840, Montana State University, Bozeman, Montana 59717-3840, USA*
[2]*Escola de Engenharia de Lorena - USP, P. O. Box 116, Lorena-SP, 12602-810, Brazil*
[3]*NIST Center for Neutron Research, National Institute of Standards and Technology, Gaithersburg, Maryland 20899-8562, USA*

(Dated: June 23, 2011)

The crystallographic structure of quasi-one-dimensional lithium purple bronze (LPB) was investigated using neutron powder diffraction (NPD) at temperatures T in the range 5 K $< T <$ 295 K. It has a monoclinic symmetry with space group $P2_1/m$, lattice parameters at 295 K are a = 12.7530(4) Å, b = 5.5239(1) Å, c = 9.4909(2) Å, and $\beta = 90.588(2)^\circ$. The sample stoichiometry was determined through chemical analysis *and* refinement of the NPD data to be $Li_{0.924}Mo_6O_{17}$ The linear thermal expansion of the lattice parameters agrees with previously reported high-resolution dilatometry measurements. The bond-valence-sum method was applied to calculate the valence of each Mo ion as a function of T, which allows discussion of the mechanism by which charge is transferred between the double one-dimensional (1D) conducting chains.

PACS numbers: 74.25.Bt, 65.40.De, 65.40.Ba
Keywords: Purple Bronze, Quasi-one-dimensional, Neutron diffraction, crystal structure

I. INTRODUCTION

The MoO_6 octahedra of molybdenum oxides are well-known to share their edges to form Mo-O chains.[1,2] The lithium purple bronze (LPB), with the approximate stoichiometry $Li_{0.9}Mo_6O_{17}$, is one such example. It is a quasi-one-dimensional (1D) metallic conductor, characterized by conducting chains that run along its b axis.[3] This material has attracted considerable attention due to the possibility that it exhibits Luttinger-liquid behavior. Photoemission experiments,[4] band-structure calculations,[5,6] power-law behavior[7] of the electrical resistance, and tunneling experiments[8] are consistent with its classification as a Luttinger-liquid metal.[9] However, the occurrence of superconductivity below ∼1.9 K was unexpected for a 1D material and the change from metallic to semiconductor-like behavior near ∼28 K was sometimes interpreted as the formation of a charge- or spin-density wave.[10] There is no direct evidence of a charge-density wave gap, though the optical conductivity does decrease near 28 K, signaling charge localization.[11] The possible existence of a charge- or spin-density wave was also addressed by high-resolution thermal-expansion experiments which suggest that a dimensional crossover occurs near 28 K. This crossover offers an explanation of why a quasi-1D material like the LPB exhibits superconductivity, which is a three-dimensional phenomenon.[12]

The electrical transport properties of this compound continue to reveal surprises. Recently, the electrical resistance as a function of temperature was fitted using two Luttinger-liquid anomalous exponents, each associated with a distinct one-dimensional band.[7] This simple fit was able to account for the temperature range 2 K $< T <$ 300 K, including the upturn from metallic to insulating behavior near 28 K. The superconductivity of the LPB is rather complex. Although modest magnetic fields destroy superconductivity,[13] magnetic fields above 30 tesla cause its reappearance.[14] Furthermore, the superconductivity is easily destroyed by disorder, and Bose-metal behavior is observed instead.[7]

The array of complex behavior exhibited by the LPB, and uncertainty regarding the role of structure and disorder in its physical properties, led us to undertake this investigation of its structure using neutron powder diffraction (NPD). The crystallographic structure of the LPB was first determined at room temperature by Onoda *et al.* using single-crystal x-ray diffraction.[2] According to their study, the structure is monoclinic with space group $P2_1/m$. NPD offers a distinct advantage over x-ray diffraction through the significantly larger neutron scattering length for oxygen, which enhances the ability to establish oxygen positions and occupancies. Performing refinements of our diffraction patterns in concert with chemical analysis, has allowed us to revise the composition of the LPB from $Li_{0.9}Mo_6O_{17}$ to $Li_{0.924}Mo_6O_{17}$. In addition, improved knowledge of the Mo-O bond lengths was used to refine calculations of the Mo valences obtained through application of the bond-valence-sum method. The temperature dependence of the Mo valences reveals a mechanism by which this compound crosses over to higher dimension at low temperature.

II. EXPERIMENTAL DETAILS

Single crystals were grown using the temperature-gradient flux method.[12,15] Approximately 2000 individually-chosen single crystals were ground using an agate mortar and pestle to obtain 2 g of powder. Atomic absorption spectrometry was performed using a Perkin Elmer Analyst 800 to determine the average Li content, which was found to be 0.924(9). NPD measurements were conducted using the BT-1 (32 detector) neutron powder diffractometer at the NIST Center for Neutron Research. A Ge(311) monochromator with a 75 degree take-off angle, $\lambda = 2.0787(2)$ Å, and in-pile collimation of 15 minutes of arc were used. The sample was sealed in a vanadium container 50 mm long and 6 mm in diameter inside a dry He-filled glovebox. A closed-cycle He refrigerator was used for temperature control. Further details about the instrument are described elsewhere.[16] Data were collected in the 2θ range of 3° to 168° with a step size of 0.05° for temperatures 5 K $< T <$ 295 K. Rietveld refinements were carried out using GSAS.[17]

III. RESULTS

Neutron-diffraction patterns could be indexed based upon the previously reported[2] space group $P2_1/m$. The coherent neutron-scattering cross sections (scattering lengths) for Li, Mo, and O are 0.454 (-1.90), 5.67 (6.715), and 4.232 (5.803) barn (fm), respectively.[18] The weak scattering of Li, relative to the other atoms, led us to fix the Li occupancy at 0.924 (the value obtained from chemical analysis). The Mo and oxygen sites were constrained to be fully occupied. Isotropic thermal parameters were refined with the constraint that they be identical for each element. Only data between $10 \leq 2\theta \leq 156$ were used in the refinement because of the absence of discernable diffraction peaks outside of this 2θ range. The final refinement was carried out for about 3000 reflections, leading to the agreement factors shown in Table I. The residuals suggest good agreement between observed and calculated profile patterns. Definition of the Rietveld-refinement agreement factors can be found elsewhere.[19]

For the 20 K data set, we allowed GSAS to determine the oxygen occupancies in order to test whether or not $Li_{0.924}Mo_6O_{17}$ has a tendency toward oxygen vacancies. GSAS calculated oxygen occupancies that were mostly a few percent above full occupancy, yielding a total oxygen occupancy of 17.7(4); only the O6 and O10 sites displayed occupancies below 1 (by 2% and 7%, respectively). Since occupancies greater than 1 are unphysical, and the total occupancy is above 17, we believe that all oxygen sites are fully occupied, in so much as GSAS is able to determine occupancies for this complex crystal structure with 12 independent oxygen sites.

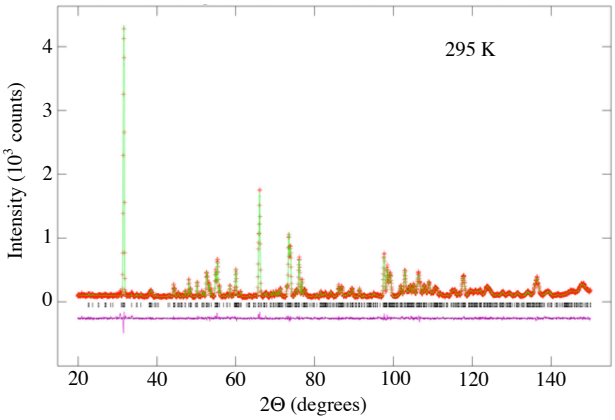

FIG. 1: (Color online) Observed (crosses) and calculated (solid line) neutron-diffraction profile for $Li_{0.924}Mo_6O_{17}$ at 295 K. The difference between these curves (i.e. the residuals) is shown as the solid line below the data/calculation and the tick marks denote the position of each reflection.

Examples of the data and Rietveld refinements at 5 and 295 K are shown in Fig. 1; the crosses represent the observed intensities and the solid lines are calculated patterns. The $P2_1/m$ space group provided excellent fits for all temperatures, in agreement with the work of Onoda *et al.*[2] No additional peaks, which could indicate the presence of superstructures or departure from the mentioned symmetry, were observed in the patterns. Also, analysis at 14 different temperatures revealed only subtle changes in the structure. In particular, diffraction data were collected at

TABLE I: Atomic coordinates, and profile agreement factors at 5 K and 295 K.

		x		y		z	
Atom	Wyckoff	5 K	295 K	5 K	295 K	5 K	295 K
Li	2e	0.4029(28)	0.4045(33)	0.75	0.75	0.3912(33)	0.4150(40)
Mo1	2e	-0.0088(8)	-0.0096(10)	0.25	0.25	0.2332(9)	0.2334(10)
Mo2	2e	0.1450(7)	0.1446(9)	0.75	0.75	0.4202(9)	0.4167(11)
Mo3	2e	0.3100(7)	0.3114(9)	0.25	0.25	0.5695(9)	0.5677(10)
Mo4	2e	0.1665(7)	0.1645(9)	0.25	0.25	-0.0795(9)	-0.0810(11)
Mo5	2e	0.3219(8)	0.3209(10)	0.75	0.75	0.0926(9)	0.0956(10)
Mo6	2e	0.4937(8)	0.4965(10)	0.25	0.25	0.1955(9)	0.1942(10)
O1	2e	0.0949(9)	0.0922(12)	0.25	0.25	0.0890(10)	0.0892(12)
O2	2e	0.5389(8)	0.5379(11)	0.25	0.25	0.0190(11)	0.0223(12)
O3	2e	0.5947(10)	0.5945(12)	0.25	0.25	0.3129(10)	0.3159(12)
O4	2e	0.8987(10)	0.9020(12)	0.25	0.25	0.4063(10)	0.4080(12)
O5	2e	0.2274(9)	0.2309(12)	0.75	0.75	0.2376(11)	0.2364(13)
O6	2e	0.7432(10)	0.7430(12)	0.75	0.75	0.2644(11)	0.2590(13)
O7	2e	0.5506(8)	0.5509(10)	0.75	0.75	0.4376(11)	0.4356(12)
O8	4f	0.0741(5)	0.0724(7)	0.5021(17)	0.5095(20)	0.3459(8)	0.3413(8)
O9	4f	0.4116(6)	0.4115(8)	0.5120(15)	0.5110(18)	0.2223(7)	0.2205(8)
O10	4f	0.2680(6)	0.2675(8)	0.5019(17)	0.5031(19)	-0.0049 (7)	-0.0032(8)
O11	4f	0.9118(7)	0.9154(9)	0.4975(15)	0.4917(19)	0.1535(7)	0.1522(8)
O12	4f	0.2716(6)	0.2707(8)	0.5046(16)	0.5100(19)	0.4722(7)	0.4751(8)
R_P (%)		5.71	6.31				
R_{WP} (%)		7.25	7.95				
χ^2		1.427	1.073				

a large number of temperatures below 50 K in order to investigate the region near 28 K that is sometimes attributed to a charge- or spin-density wave.[11,12]

Atomic coordinates at 5 and 295 K are listed in Table I. The crystal structure of $Li_{0.924}Mo_6O_{17}$ is displayed in Fig. 2. It was calculated using the program JAVA STRUCTURE VIEWER[20] and the room temperature data of Table I. The unit cell contains six independent molybdenum sites. Two Mo ions, labeled Mo3 and Mo6, are located in MoO_4 tetrahedra while the remaining four are in MoO_6 octahedra. Tetrahedra (for one Mo3 and one Mo6 ion only) and the octahedra (Mo1, Mo2, Mo4, and Mo5 only) are shown in the figure for two adjacent quasi-1D planes. Notable is the fact that MoO_4 tetrahedra terminate the quasi-1D planes, which extend along the b axis and are perpendicular to the $[\bar{1}02]$ direction. The quasi-1D planes are defined in the a-c plane by the sequence Mo3-O12-Mo2-O8-Mo1-O11-Mo4-O10-Mo5-O9-Mo6, which lies along the [101] direction. The well-known Mo1-O11-Mo4 double 1D zig-zag chains run along the b axis[1,2,6] at the center of the quasi-1D planes. They can be seen in Fig. 2, highlighted by the green lines. The zig-zag chains are thought to be the most electrically conducting component of $Li_{0.924}Mo_6O_{17}$. This was surmised from the ionic valences that were extracted through a bond-valence sum analysis[2] (discussed below) and band structure calculations.[5,6] Directly above and below the double layers of 1D zig-zag chains are the Mo2 and Mo3 ions, which occupy one side of the quasi-1D planes. On the other side of these planes are the Mo5 and Mo6 ions. Li atoms are located at the ends of the quasi-1D planes, and are collinear with Mo3 and Mo6 along the crystallographic $[\bar{1}02]$ direction. In this particular region, the quasi-1D planes are highly distorted.

Figure 3 shows the temperature dependence of the lattice parameters a, b, and c. The results reveal strongly-anisotropic behavior. The a and b lattice parameters contract with decreasing temperature. However, along the c axis, a contraction from room temperature down to ∼220 K is followed by an expansion with further cooling. We found no evidence of a structural distortion near 28 K, strengthening the viewpoint that the transition in the electrical resistivity in this region is not a consequence of a traditional charge- or spin-density wave.[11,12] Note that a *purely electronic* charge- or spin-density wave might still be present.[12] Figure 3 also compares these results to thermal expansion (dilatometry) data[12] by scaling the latter by the respective lattice parameter; the thermal expansion data appear as a thin line, although approximately 1700 individual data points make up each data set. The agreement between the thermal expansion and lattice parameters versus temperature data is good. Selected interatomic distances

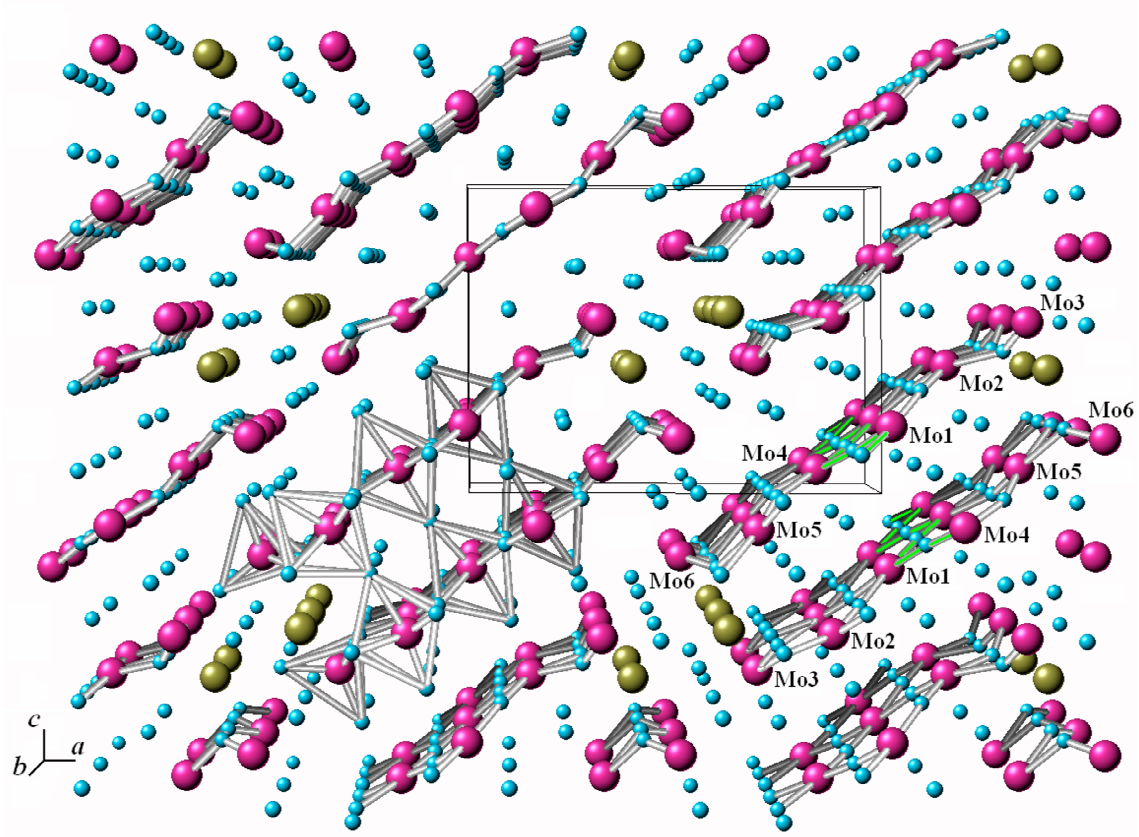

FIG. 2: (Color online) Illustration of the crystallographic structure for $Li_{0.924}Mo_6O_{17}$ based upon the data of Table I at 295 K. Mo ions are magenta, oxygen ions are light blue, and Li ions are dark yellow. Evident is a structure composed of quasi-1D planes that terminate in the vicinity of the Li ions. This is best appreciated by viewing the planes with MoO_6 octahedra drawn in (lower left). MoO_4 tetrahedra terminate the quasi-1D planes on both sides. A number of the quasi-1D planes are drawn without the octahedra and polyhedra to emphasize the planar nature. The box near the center of the figure indicates the unit cell. Two zig-zag chains are shown in green, near the lower-right-hand side of the box. JAVA STRUCTURE VIEWER was used to create the figure.[20]

at 295 K are listed in Table II. We made plots of the Mo-O bond lengths versus T and angles as a function of temperature (not shown), but failed to find any distinctive behavior. For this reason, these plots are not shown.

To better understand the roles of the individual Mo ions in the conduction process, the molybdenum-oxygen bond lengths were used to determine the molybdenum valences with the bond-valence-sum method. Here, the bond lengths are used to calculate the bond valences using empirical parameters.[21,22] The resulting valence of cation i, V_i, is given by summing the bond valences S_j for each bond according to

$$V_i = \sum_j (S_j) = \sum_j \exp[(L_o\text{-}L_{ij})/B]. \quad (1)$$

In Equation (1) L_o and B are empirically determined[22] (we have used $L_o = 1.900$ Å and $B = 0.37$ Å) and L_{ij} are the actual bond lengths between i and j molybdenum and oxygen ions, respectively. A similar analysis was done previously,[2] but refinements to the bond-valence sum method[22] and our improvements in the measured bond lengths led us to revisit this analysis. The obtained bond valences and Mo valences are listed in Table III for 295 K. The values are slightly different from those obtained by Onoda *et al.*[2] This can be partially attributed to the L_o and B values used in that reference, which have since been refined.[22]

The temperature dependence of the Mo valences is displayed in Figure 4. The average of the Mo valences from the bond-valence-sum analysis (5.7(4)) at 295 K is higher than the value of 5.51 that is expected for the LPB composition ($Li_{0.924}Mo_6O_{17}$). It is important to mention that a value of 6 for the Mo valence would imply that the Mo ion has transferred its electrons to the neighboring oxygen ion and does not contribute to electrical conduction. Note that Hall effect measurements and band structure studies reveal holes as the charge carriers.[6,23]

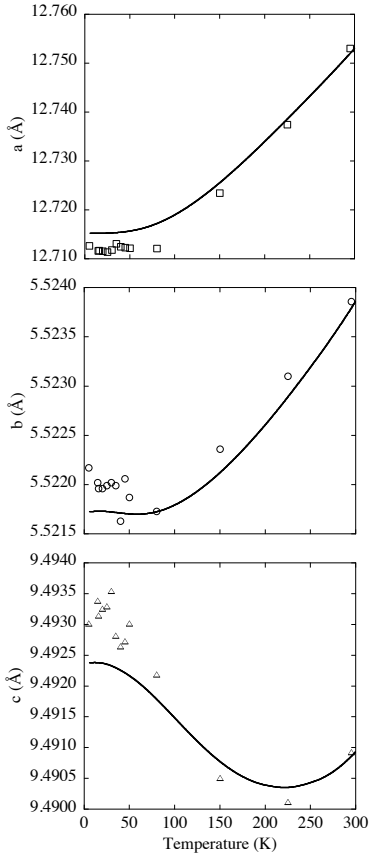

FIG. 3: Lattice parameters as a function of temperature. Error bars are smaller than symbols. Notable is the highly anisotropic behavior and the relatively large change of the a-axis lattice parameter. Solid lines are actually linear thermal expansion data taken at 0.2 K intervals, with approximately 1700 data points in each curve. These data are from dos Santos et al.[12]

TABLE II: Selected interatomic distances (Å) at 295K. The notation (x2) means that there are 2 Mo-O bonds in the unit cell.

Bond	295 K	***Bond***	295 K
Li-O3	2.55(4)	Mo3-O6	1.792(17)
Li-O5	2.78(4)	Mo3-O7	1.756(18)
Li-O7	1.88(4)	Mo3-O12 (x2)	1.759(11)
Li-O9 (x2)	2.27(4)	Mo4-O1	1.868(16)
Li-O12 (x2)	2.24(4)	Mo4-O6	2.071(19)
Mo1-O1	1.896(16)	Mo4-O10 (x2)	2.051(12)
Mo1-O4	2.014(17)	Mo4-O11 (x2)	1.875(14)
Mo1-O8 (x2)	2.043(13)	Mo5-O2	2.129(17)
Mo1-O11 (x2)	1.810(13)	Mo5-O5	1.771(19)
Mo2-O4	1.772(16)	Mo5-O9 (x2)	2.110(12)
Mo2-O5	2.044(18)	Mo5-O10 (x2)	1.786(12)
Mo2-O8 (x2)	1.764(13)	Mo6-O2	1.720(17)
Mo2-O12	2.152(14)	Mo6-O3	1.692(18)
		Mo6-O9 (x2)	1.823(12)

TABLE III: Bond valences and molybdenum valences at 295 K obtained using the bond-valence-sum method.

	Mo1	Mo2	Mo3	Mo4	Mo5	Mo6
O1	1.01(3)			1.09(3)		
O2					0.54(2)	1.63(5)
O3						1.75(5)
O4	0.73(2)	1.41(4)				
O5		0.68(2)			1.42(4)	
O6			1.34(4)	0.63(2)		
O7			1.48(4)			
O8	0.68(2)	1.44(4)				
O9					0.57(2)	1.23(4)
O10				0.67(2)	1.36(4)	
O11	1.27(4)			1.07(3)		
O12		0.51(1)	1.46(4)			
Mo	**5.7(2)**	**6.0(2)**	**5.7(2)**	**5.2(2)**	**5.8(2)**	**5.8(2)**

The results in Table III and the upper panel of Figure 4 show that Mo2 and Mo3 have valences near 6, and therefore do not contribute significantly to electrical conduction. In this region of the quasi-1D planes, the Mo1 valence remains distinctly lower than the Mo2 and Mo3 valences for all temperatures. This suggests that Mo2 and Mo3 do not play significant roles in electrical conduction for the temperature range of this work. On the other side of the quasi-1D planes, the story is quite different. Near room temperature, Mo5 and Mo6 have slightly higher valences than Mo4, and hence a lower contribution to the electrical conductivity. However, this relationship changes as the temperature is lowered. The Mo4 valence increases slightly, while the Mo5 and Mo6 valences decrease slightly. The similarity in the valences for Mo4, Mo5, and Mo6 below 30 K indicates that the assumption of electrical conduction as primarily occurring along the Mo1-O11-Mo4 double 1D zig-zag chains may no longer be valid in this temperature region.

Previous work has discussed the crossover[12] from quasi-1D to higher dimension in $Li_{0.924}Mo_6O_{17}$. The results of the bond-valence-sum analysis (see Figure 4) enable us to discuss a possible mechanism for this crossover. In appreciating this scenario, it is important to keep in mind that the zig-zag chains occupy two adjacent quasi-1D planes, coupling the planes to one another. Although the double zig-zag chains are adjacent to the Mo2 and Mo3 ions in neighboring quasi-1D planes, the data of Figure 4 (upper panel) suggest that there is little charge transfer between these ions and the zig-zag chains. On the other hand, the data in the lower panel of Figure 4 indicate that Mo5 and Mo6 play an increasingly important role in the conduction mechanism as temperature is reduced, with valences at low temperature that are similar to the Mo4 valence. Inspection of Figure 2 reveals that the Mo5 and Mo6 ions at the end of adjacent quasi-1D planes are bridged by the O2 ions along the c direction. Thus, increased overlap of Mo5 and Mo6 ions via the O2 ions will lead to a more three-dimensional behavior by coupling the networks of double quasi-1D planes to one another. Furthermore, the exceptionally strong thermal contraction with cooling[12] along a, which leads to a large thermal contraction along the $[\bar{1}02]$ direction, is the most likely change in structure that causes the crossover since it would enhance the overlap in this region of the crystal structure. The fact that these changes in crystal and electronic structure are very subtle, is probably the reason why $Li_{0.924}Mo_6O_{17}$ still retains strongly low-dimensional behavior, even at low temperature, as evidenced by the very anisotropic superconducting properties, appearance of Bose metal behavior[7], and occurrence of reentrant superconductivity.[14]

IV. CONCLUSIONS

In summary, new information about the chemical composition, crystal structure, and dimensionality of $Li_{0.924}Mo_6O_{17}$ has been reported. The Li composition was determined based upon chemical analysis and the oxygen composition was then refined in the structural calculations. The results reveal the composition of $Li_{0.924}Mo_6O_{17}$. Rietveld refinements of the NPD were conducted at 14 temperatures from 5 K to 300 K in order to investigate the influence of temperature on the crystal structure. Only subtle changes in the structure were observed. Because of this, we conducted a bond-valence-sum analysis using the Mn-O bond lengths. This revealed that the Mo valences exhibit temperature dependent changes that indicate a mechanism for the dimensional crossover that was previously reported.[12] The mechanism appears to be electronic overlap of quasi-1D planes on the edges where the Mo5 and

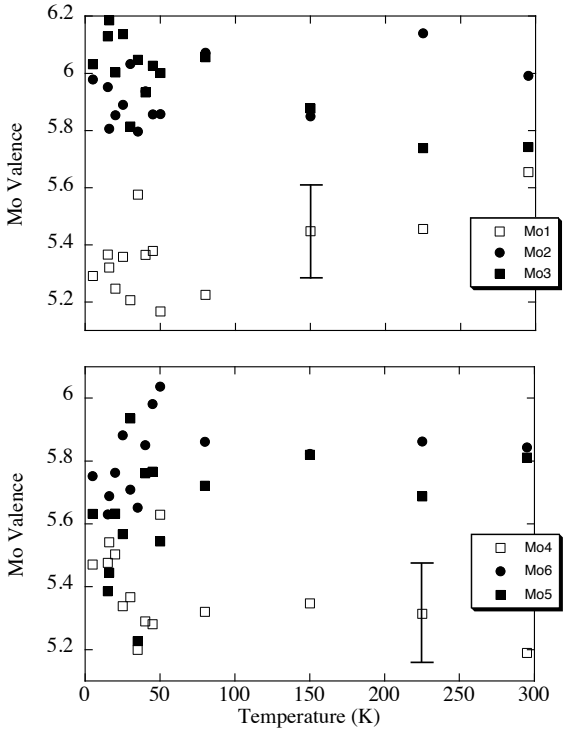

FIG. 4: Mo valences determined using the bond-valence sum method are presented as function of temperature for the six Mo ions in $Li_{0.924}Mo_6O_{17}$. The top panel shows data for Mo1, Mo2, and Mo3, representing one side of the quasi-2D planes, which the lower panel shows data for Mo4, Mo5, and Mo6, representing the other side of the quasi-2D planes. The error bar was estimated based upon the standard deviation.

Mo6 ions reside. The results reported here provide new insight into the highly anisotropic electrical behavior of the $Li_{0.924}Mo_6O_{17}$. Furthermore, the structural information reported herein will prove valuable for future investigations.

V. ACKNOWLEDGEMENTS

This material is based upon work supported by the U.S. Department of Energy Office of Basic Energy Sciences (DE-FG-06ER46269), the National Science Foundation (DMR-0504769 and DMR-0907036), FAPESP (2009/14524-6), and CNPq (301334/2007-2 and 490182/2009-7). The authors thank Judith Stalick for her gracious assistance with the data files, and Christopher Ling for answering numerous questions regarding GSAS.

* Permanent Address: Instituto de Ciências Tecnológicas e Exatas, Universidade Federal do Triângulo Mineiro - UFTM, CEP: 38025-180 - Uberaba - MG, Brazil.

[1] T. Hughbanks and R. Hoffmann, J. Am. Chem. Soc. **105**, 3528 (1983).
[2] M. Onoda, K. Toriumi, Y. Matsuda, and M. Sato, J. Solid State Chem. **66**, 163 (1987).
[3] M. S. da Luz, C. A. M. dos Santos, J. Moreno, B. D. White, J. J. Neumeier, Phys. Rev. B **76**, 233105 (2007).
[4] Feng Wang, J. V. Alvarez, S.-K. Mo, J. W. Allen, G.-H. Gweon, J. He, R. Jin, D. Mandrus, and H. Höchst, Phys. Rev. Lett. **96**, 196403 (2006).
[5] M. H. Whangbo and E. Canadell, J. Am. Chem. Soc. **110**, 358 (1988).
[6] Z. S. Popović and S. Satpathy, Phys. Rev. B **74**, 045117 (2006).
[7] C. A. M. dos Santos, M. S. da Luz, Yi-Kuo Yu, J. J. Neumeier, J. Moreno, and B. D. White, Phys. Rev. B **77**, 193106 (2008).
[8] J. Hagen, R. Matzdorf, J. He, R. He, R. Jin, D. Mandrus, M. A. Cazalilla, and E. W. Plummer, Phys. Rev. Lett **95**, 186402 (2005).
[9] J. Voit, Rep. Prog. Phys. **58**, 977 (1995).
[10] M. Greenblatt, W. H. McCarrol, R. Neifeld, M. Croft, and J. V. Waszczak, Solid State Comm. **51**, 671 (1984).
[11] J. Choi, J. L. Musfeldt, J. He, R. Jin, J. R. Thompson, D. Mandrus, X. N. Lin, V. A. Bondarenko, and J. W. Brill, Phys. Rev. Lett. **69**, 085120 (2004).
[12] C. A. M. dos Santos, B. D. White, Yi-KuoYu, J. J. Neumeier, and J. A. Souza, Phys. Rev. Lett. **98**, 266405 (2007).
[13] C. Schlenker, H. Schwenk, C. Escribe-Filippini, and J. Marcus, Physica B **135B**, 511 (1985).
[14] X. Xu, A. F. Bangura, J. G. Analytis, J. D. Fletcher, M. M. J. French, N. Shannon, J. He, S. Zhang, D. Mandrus, R. Jin, and N. E. Hussey, Phys. Rev. Lett. **102**, 206602 (2009).
[15] W. H. McCarroll, and M. Greenblatt, J. Solid State Chem. **54**, 282 (1984).
[16] http://www.ncnr.nist.gov/
[17] A. C. Larson and R. B. von Dreele, General Structure Analysis System (GSAS), Los Alamos National Laboratory Report No. LAUR 86-748 (1994).
[18] see: www.ncnr.nist.gov/resources/n-lengths/.
[19] L. B. McCusker, R. B. Von Dreele, D. E. Cox, D. Louer, and P. Scardi, J. Appl. Crystallogr. **32**, 36 (1999).
[20] S. Weber, J. Appl. Crystallogr. **32**, 1027 (1999).
[21] I. D. Brown and D. Altermatt, Acta Cryst. B **41**, 244 (1985).
[22] I. D. Brown, Chem. Rev. **109**, 6858 (2009).
[23] H. Chen, J. J. Ying, Y. L. Xie, G. Wu, T. Wu, and X. H. Chen, Euro. Phys. Lett. **89**, 67010 (2010).